Geometric Electrode Effects on the Induced Photocurrent in Polycrystalline Diamond Based X- Ray Dosimeters

K.S.AL Mugren[1,2]

1.Center for Nuclear and Radiation Physics, Department of Physics, University of Surrey, Guildford, GU2 7XH, United Kingdom

2.Permanent address: Physics Department, Faculty of Sciences, Princess Nourah Bint AbdulRahman University, Riyadh, KSA

* E-mail of the corresponding author: ksalmogren@pnu.edu.sa

Abstract

The aim of the study is to develop tissue equivalent CVD diamond based dosimeters with a carbon based electrodes. We have initially studied the dependence of induced X-ray photocurrent amplitude and time response as a function of electrode area under broad beam X-ray irradiation. For this purpose, we have fabricated circular electrode sandwich tested structures based on thermal grade polycrystalline CVD diamond with different 3 diameters. The X-ray photocurrent increases with increasing dose rate sub linearly. Although the photocurrent increases with increasing electrode diameter, the increase in current is less than expected from the increase in active area. To further investigate, a small detector based upon 4 separate circular pad was tested for sensitivity with respect to detector area, applied bias voltage and incident x-ray doserate. Additionally the rise time of these detectors was evaluated with respect to the same criteria from these tests there was a non-linear relationship of under response between detector area and sensitivity under broad beam irradiation, the cause of which has been attributed to edge effects, supported by the results from collimated beam measurements. The results from the rise time tests appear to indicate that the time dependent components of the detector response are affected primarily by the applied bias upon the detector and the quality of the material, with additional doserate related effects scaling with bias. The higher quality material was found to have a far greater dependence on applied bias than the lower quality sample, which varied little.

Keywords: CVD Diamond, Dosimetric Characteristic, Electrical Contact, Radiation Detector, Thermal Grade polycrystalline diamond.

Introduction

Diamond is a very interesting material with many exotic properties. The large band gap, radiation hardness, optical transparency, large saturated carrier velocities and low atomic number of diamond all make it a very attractive candidate for applications in radiation detection. (.Manfredotti, C., et al, 1998) In addition, Diamond is a very radiation hard material due to the strength of sp^3 bonds between carbon atoms. This gives potential for diamond in extreme harsh environments like nuclear reactors, accelerators and space applications. In medical applications, diamond is a promising material because its Z number is very close to that for human body tissue (6 and 7 respectively)(Guerrero, M.J., et al 2004, Knoll, G.F. 2010). Also, it's inertness makes it safe material. Due to its physical properties, diamond is of great interest for use as a detector material. It has a robust structure of chemical bonds leading to exceptional hardness to damage from ionizing radiations and chemical reactions, it has an atomic number (Z henceforth) of 6 when compared to an effective Z of 7.4 for muscle and 5.92 for fat (Attix, F., et al 1968) resulting in superior tissue equivalence for dosimetry compared to its alternatives such as silicon. Diamond possesses a relatively wide band gap of 5.4eV, allowing use as a solid-state ionisation chamber which is relatively insensitive to visible light with low noise at room temperature, though this relatively wide band gap also sacrifices energy resolution in spectroscopic applications (Manfredotti, C., et al, 1998). Diamonds also have additional applications as a thermoluminesent dosimeter (Guerrero, M.J., et al 2004) as a consequence of deep traps in the electronic band structure of the material. Many of these properties are already exploited in diamond detectors based on highly selected natural diamonds, but suitable samples are rare and thus, particularly expensive. As a consequence of this, there is particular interest in artificially produced diamond for dosimetry purposes. With modern synthesis processes based on chemical vapour deposition, the resulting diamonds could prove to be both cheaper and better suited to dosimetry purposes if properly characterised, particularly for the single crystal types of diamond. There are additional upsides in that the consistently producible material may also be tailored for a specific application by manipulating the levels of impurities, such as nitrogen,(Schirru, F., et al 2007). The nature of the synthesis process for polycrystalline samples permits the production of a versatile range of geometries. This ranges from thin films for wider area detectors down to very small but usefully sensitive samples grown onto a small tip, to improve spatial resolution. The previously mentioned lower Z value and capacity for manufacture of thin films also suggests that diamond would make a better transmission mode detector, particularly with carbon type electrodes employed, when compared with silicon or other heavier semiconductors. There has been significant development in the field of synthetic diamond dosimeters of both the

thermoluminescent and direct measurement type and several geometries have been studied in the literature. Some of the common findings can be summarised as follows. For applications as an offline thermoluminescent detector manipulating the nitrogen concentration is the main way of influencing its response, particularly for the applications with single crystal diamonds (Guerrero, M.J., et al 2004, Schirru, F., et al 2007). That for use as a solid state ionisation chamber detector grade diamond is sufficient to produce a useful dosimeter provided it is properly encapsulated, and can even be found to be superior or competitive with natural diamonds ion chambers and silicon diodes for selected energy ranges (Guerrero, M.J., et al 2004, Manfredotti, C. 2005, Manfredotti, C., et al, 2001, Lansley, S., et al 2011, Buttar, C.M., et al 1997, Betzel, G.T., et al 2010, Almaviva, S., et al 2009, Bruzzi, M., et al 2004). It is almost always concluded that the priming effects of diamond are a limiting factor in their suitability, but once primed it is a suitable material (Guerrero, M.J., et al 2004, Manfredotti, C. 2005, Bruzzi, M., et al 2004, Whitehead, A.J., et al 2001, Marczewska, B., et al 2001, Lei, L., et al 2012, Adea, N., et al 2014). As a material for dosimeters single crystal diamond will exhibit better linearity due to the distributions of traps, with near perfect values achievable (Betzel, G.T., et al 2010) , whereas polycrystalline samples generally have lower values (Marczewska, B., et al 2001) due to the grain boundaries. Rise times have been found to vary with both applied bias and exposure, increasing with respect to the first, and dropping with dose rate (Betzel, G.T., et al 2010). When operated in photovoltaic mode, single crystal-based detectors are found to have rise times comparable to ionization chambers (Almaviva, S., et al 2009). The scope of this work is to extend the method to the characterization of Poly Crystalline CVD diamond metalized using a metal contact (Aluminium) (PC(AL)) with three circles of diameters 2, 3.9 and 5.9 mm, and to show the different between them with I-V measurements, X- ray photo current, the delta value (the deviation from linearity at fowler's equation) and the Time response (rise time and fall-off time). This work looks at the effects upon various performance parameters for a film type polycrystalline diamond sample deposited with symmetrical sets of circular pads, effectively creating 3 detectors of very similar parameters except for a variation in active area as determined by the contacts. The parameters investigated include the relative sensitivity, linearity, repeatability, and time dependent response effects as functions of the detector area, incident x-ray flux and detector bias. For purposes of comparison some of these tests were also repeated upon a second, smaller diamond film sample with a set of different sized contacts upon it. The response with respect to area of this detector in a different mounting configuration was the motivation for this piece of work; to investigate whether the observed effects were unique to that particular sample or related to some underlying systematic process.

1.   Experimental methodology

The detector was manufactured on a polycrystalline CVD diamond with dimensions (3x(5,4,2mm)for (Sample.2), which was produced by(ELEMENT SIX LTD (UK). The sample was cleaned with 60 ml of hydrochloric acid (HCl) and 20 ml of nitric acid (HNO$_3$). Then, both the top and the back surfaces were metalized by thermal evaporation with 100 nm thick of aluminium (AL) with three circles of diameters (5mm, 4mm and 2mm). The device was mounted on printed circuit board (PCB) with dimension ((2.2 x 1.6) cm^{2}and 1 mm thick) using a small dot of gold paste on the centre of the three deposited circles. Three gold wires (25 μm thickness) bond are fixed on the top of three circles contact using Conductive Silver Epoxy. This was done by using a microscope, the tip of the wire holding the very small amount of glue was lowered on top of the AL contact and secured there for 3 hours until the glue had dried. The other end of the gold wires was connected to their corresponding copper pads on the PCB using silver paint. In same steps, Sample.1 was manufactured on a polycrystalline CVD diamond with dimensions 4x(7,6,6,5mm). Figure1. has shown the four devices (Sample.1) and three devices (Sample.2), The pads are connected with standard electrical wires connected to a BNC bulkhead connector, which controls which device will be measured by changing which of the wires is connected to the port. A fourth wire is used as a ground device. During the measurements and analysis, the pads on each detector have each been referred to by a single letter, as shown in Figure 1. The letters A-D correspond with the pads on the larger sample; labelled clockwise from the largest pad such that A, B, C, and D correspond. with pads of 7, 6, 5, and 6 mm diameter respectively. E-G correspond with the pads on sample 2 and are simply allocated in biggest-smallest order, so E, F, G correspond to pads of 5, 4, and 2 mm diameter respectively. Table.1 has Summarized the information about diamond samples were used.
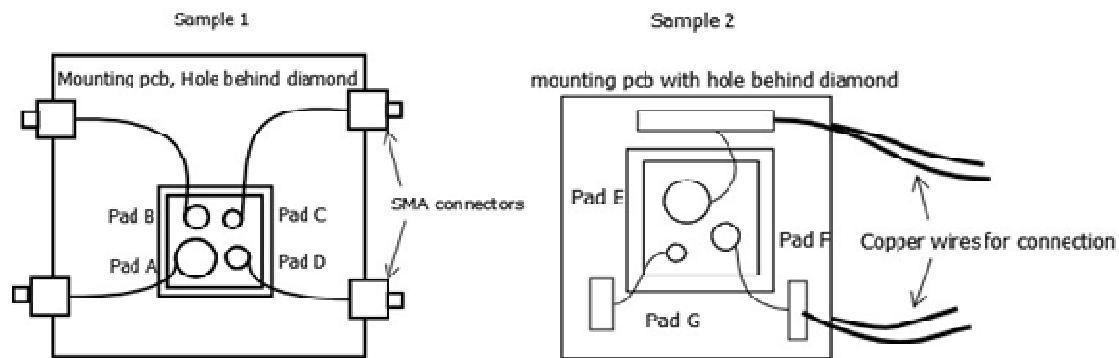
Figure 1. *Diamond samples(1&2) as used in the experiment.*

Table 1. *Summary table of information about diamond sample used.*

Sample	Material	area	thickness	Pads
1	Detector quality	20mmx20mm	0.3mm	4x(7,6,6,5mm dia)
2	Detector quality	10mmx10mm	0.5mm	3x(5,4,2mm dia)

1.1 Measurements

For all measurements taken and commented upon, the setup used was as shown in Figure.2, with the samples mounted into a metal box with a tape window to minimize light effects, and a black cloth placed over the entire setup to further reduce any light ingress. The x-ray source used was an Oxford instruments manufactured tube with a molybdenum target anode. The tube was operated at 50kVp for all measurements taken, and the tube current varied to vary the detector's incident doserate. The tubes maximum current capability of 1000µA was employed for all measurement series where tube current was to be kept constant. A range from 1000µA down to 50µA in 100µA or 50µA steps was used where tube current was the varied parameter. Due to the properties of an x-ray tubes dose output being linear with the tube current, references to doserate in the results are based on it being directly proportional with tube current, which was varied, and the distance between tube and detector, which was kept as constant as possible to provide a range of doserates to the detector. To account for the effect on apparent detector rise times that the x-ray tubes own transient response will introduce to any measurements, a silicon PIN diode, Hammatsu model s1223, was exposed at a variety of tube currents, the results of which are displayed in Figure 15 with the related diamond results. For the un-collimated measurements, the tube and detector were aligned such that the centre of the detector was roughly centred upon the square of the diamond, with no particular attention paid to centring the beam on any one pad. For the results using a collimated beam a 12cm brass tube with a 2mm hole was used, and was placed as close to the x-ray tube as was practical whilst still allowing alignment to be performed. To accomplish the required fine alignment, a bright LED was placed in front of the x-ray tube window and used to illuminate a spot on the detector through the collimator. This was then manoeuvred as close to the centre of each detector pad as possible (as judged by eye) using the adjustable mounts on the optical bench. Due to the varying time-dependent effects on the current signal under irradiation a consistent protocol for exposures was required. Based on observations from the initial familiarisation testing runs it was decided for the highest bias case that 30 seconds per exposure was sufficiently long to have achieved near stability in the response of the detector, and to still allow a practical number of measurements to be taken. The acquisition of current-time plots from the Keithly 487 picoammeter/voltage source was done using a provided LabVIEW VI known as "testbed v3". For measurements on the time-dependent effects, it was necessary to disable the default averaging across 10 readings followed a wait of 1000ms between each. To obtain a useful level of time resolution for measurements on the transients involved, the averaging was set to use only a single picoammeter reading with as little delay between measurements as low as the program would allow, resulting in a time between measurements of approximately 260ms. This change had the apparent effect on the results of increasing the noise, but is justified in that it better represents the actual noise on the detector, which is of particular interest for a dosimeter.
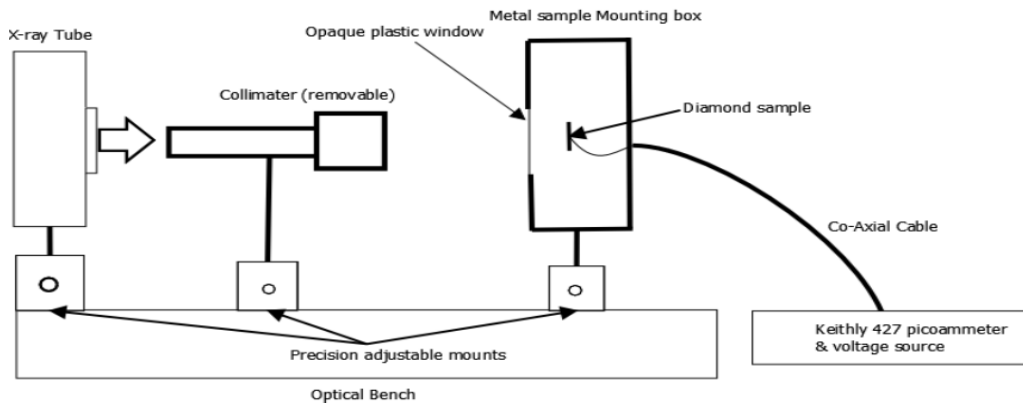
Figure 2. *Experimental apparatus as used for reported measurements.*

1.2 Data Analysis

In order to efficiently and consistently evaluate the volume of data gathered, a LabVIEW VI was constructed to do the analysis, taking the mean peak current, standard deviation in the mean and rise time in a semi-automated manner, based upon a selected data range around a peak on a displayed graph of the data, as depicted in the example in Figure 3.
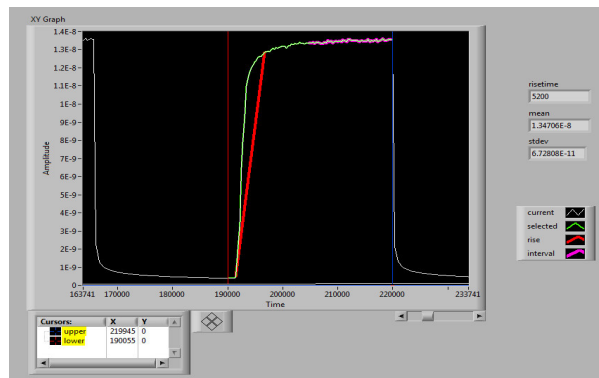
Figure 3. *Image of LabVIEW VI used to process data, showing the selected time region in green highlight and the intervals over which the mean and rise time are calculated, in purple and red respectively.*

The mean peak current measured as an average of the current amplitude over the last 15 seconds of each 30 second exposure, where the current is found to be suitably stable, defined by the manual positioning of a cursor at the time position of the clear signal transient where the current drops due to the switch off of the x-ray tube. From this mean it was then automatically calculated the 5% amplitude accounting for dark current and the 95% amplitude for which time positions are automatically calculated. The difference in these time positions is given as the rise time. The standard deviation was also taken over this interval used to calculate the mean value. After extraction of the values from the raw data, there was averaging carried out on each run of repeats to give a final set of values, with an estimate of the error and a signal-to-noise ratio.

2. Results and Discussion Measurement Reproducibility

Throughout the measurements taken for this study there were problems with random instabilities, some of which were attributed to the setup. There was found an instability with the flux that became more pronounced with bigger pads and low fields in which; during a normal exposure the signal would go from stable to having unexpected noise on a level close to that of the signal after a short time interval, though this was not found to be a reliably repeatable finding. Sample 1 was also found to, following numerous series of exposures, suddenly 'snap' and generate noise of a magnitude capable of suppressing any signals which persisted even in the absence of any incident x-rays. The only solution to this was found to be breaking off measurements for the day, after which the detector appeared stabilised from being left unbiased and un-irradiated overnight.

2.1 IV measurements

The I-V dark current measurements on each of the detector pads revealed the equipment to be working as would be expected for a high quality detector. For Sample 1, shown in Figure.4, dark currents of around 200pA at 120v bias with very little deviation were achieved once the initial issues with the mounting system generating excess noise were solved. This was found to be adequate to give usable signals across the range of doserates tested,

provided it remained stable. It can be observed that whilst the dark currents appear to follow the size of the pads in their magnitudes, the response from Pad A is not 1.3 times the responses of pads B and D, so it is not a simple linear variation with area. The results for Sample 2, as shown in Figure.5, reveal the possible inconsistencies in the quality of the material. There is a dark current roughly 12 times that of the others on the detector for the mid-sized pad. The others demonstrate a dark current smaller than that observed in the other detector at similar fields. These other pads were additionally found to demonstrate a negative dark current, so the smaller dark current at maximum here may stem from time-dependent polarization effects or similar, as there was not time to do a in-depth set of measurements on this sample.
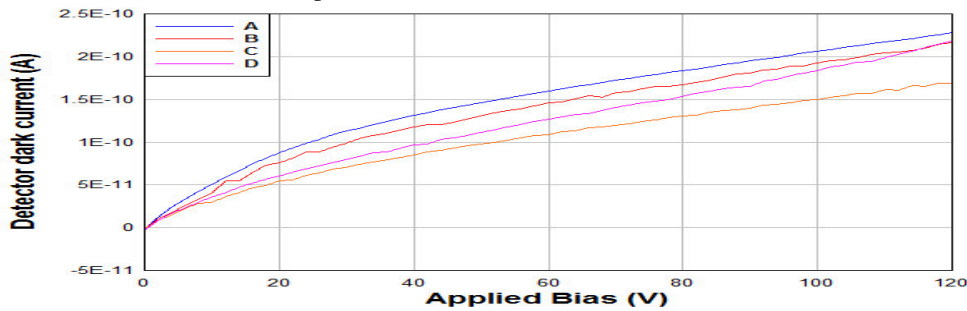
Figure 4. *Results for IV measurements on Sample1.*
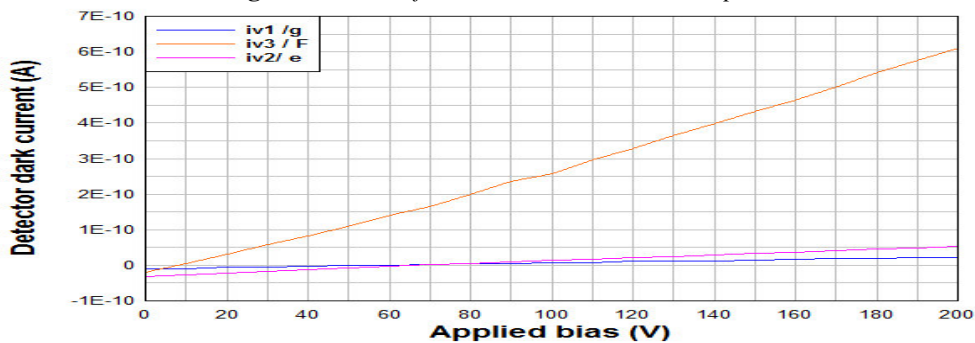
Figure 5.*Results for IV measurements on Sample 2.*

2.2 Current vs. Dose rate measurements
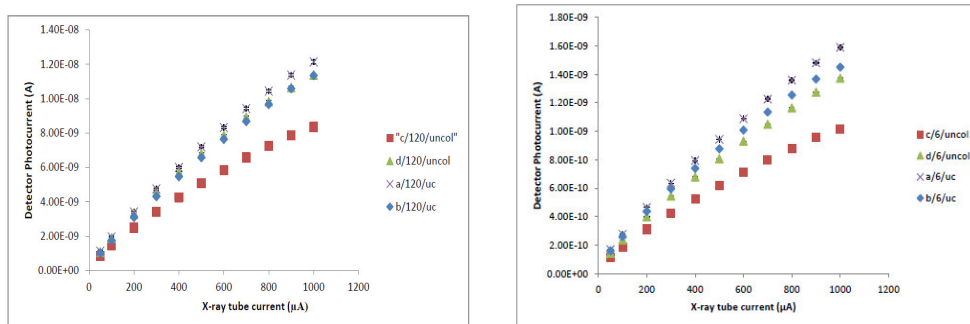
Figure 6. *Detector photocurrent vs. x-ray tube current for Sample.1 (120v bias and 60v bias), no collimator.*
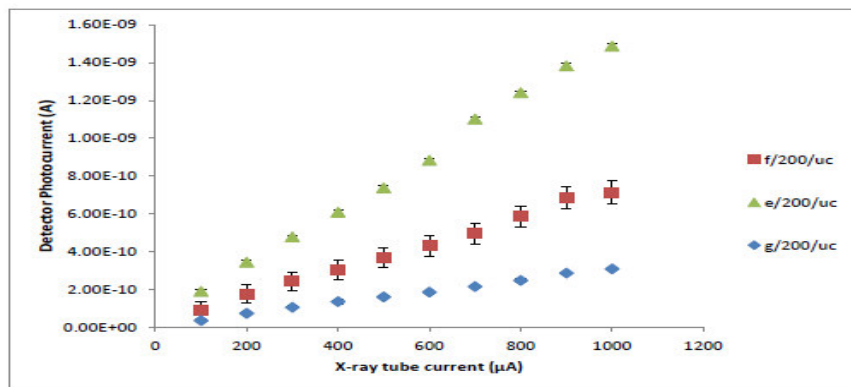
Figure 7. *Detector photocurrent vs. x-ray tube current for Sample 2 at 200v bias, no collimator.*
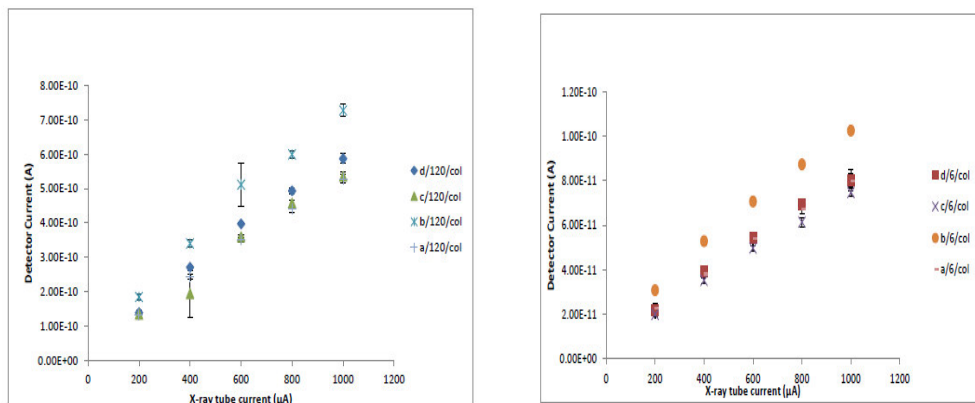
Figure 8. *Detector photocurrent vs. x-ray tube current for Sample.1 at (120v bias and 60v bias), with collimator.*
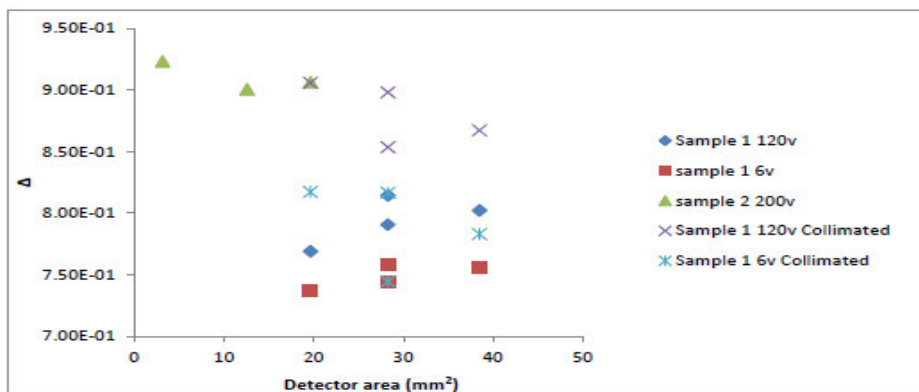
Figure 9. *Fowler fit Δ parameter with respect to area for figures 6-8.*

From the photocurrents obtained with varying x-ray tube current (to vary doserate)(Figur.6,7,8), it is seen that each pad displays a response of the expected from photocurrent in addition to the dark current increases with increasing doserate. For every pad tested across both samples, the photocurrent was found to deviate from linearity with respect to doserate across the tested range.

As predicted by the Fowler relation (**Fowler, J. F.   1966**) (For solid state ionization chambers, the Fowler relation is often used to describe the relation between the current generated and the doserate, in the form of a power law fit:

$$I = I_d + R * D_r{}^{\Delta}$$

where I is the measured current out of the device, I_d is dark current of the device, R is a scaling factor for the response, D_r the incident doserate on the device, and Δ being a measure of linearity, accounting for any deviations from linear response)., this non-linearity is quantifiable as a power fit on each current-doserate trace, the parameters of which are graphed as a function of area in Figure.9. For Sample 1 (the 4 pad, thinner, larger

14

sample) this non-linearity exponent was found to be between 0.73 and 0.81. Sample 2 (the 3 pad, thicker, smaller pad, smaller sample) was found to have an apparently better linearity with the exponent being around 0.9. From the data, there is no visible certain dependence between this value and the size of the pad. For the larger sample, there is an improvement in each case between the low bias and high bias measurements, with the higher bias having a Δ closer to 1. This can be possibly attributed to the improved charge collection characteristics and lessened recombination effects in the presence of a stronger field. As the bias voltages were chosen such that the field through each sample is equal, the improved linearity may be attributed to differences in the diamond between samples. From the collimated results there is a visible over-response of one of the medium sized pads. This result was still visible when the collimated results were repeated(Figure.8), suggesting that it is not simply a matter of misalignment of the collimated x-ray beam but a property of the detector. Potentially as a result of spatial variations of the diamond material in the pads sensitive area, which would be averaged out in broad beam irradiation or, an irregularity in the metal pads and associated wire bonds boosting sensitivity for a small spot. For the second sample it was found that the dark current for the medium sized pad was around 10 times that of the other pads, indicating similar spatial effects or fabrication defects could be involved. For the Sample 1 measurements with a collimator in place, aside from the apparent over-response of one of the pads, there is also an apparent improvement in the delta parameter, this improved linearity could simply be due to the lower doserate range studied due to the collimator leading to lesser x-ray fluxes on the detector, but could also point to edge effects in the detectors being involved, and warrants further investigation.

2.3 Current-Bias Measurements
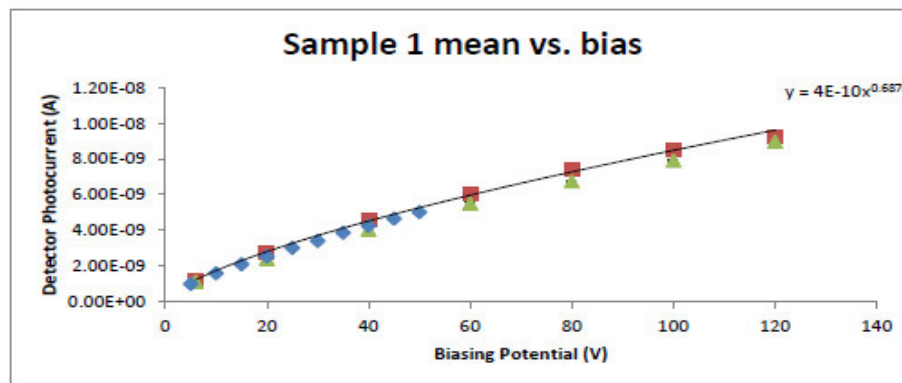
Figure 10. *Detector photocurrent vs. bias for Sample.1 pad c at 1000µA tube current, the multiple series are for results taken in different sets of measurements.*
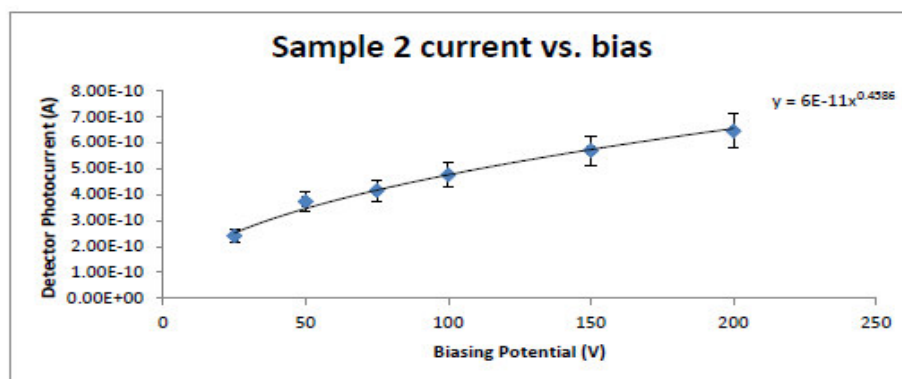
Figure 11. *Detector photocurrent vs. bias for Sample 2 pad F at 1000µA tube current.*

Figure.10 and 11, show the results as obtained from measurement of photocurrent on a single pad on Samples 1 and 2 respectively, where the incident doserate on the detector was kept constant and the applied bias varied. As is expected the current obtained from the samples increased with the applied electric field, but the response was not linear, with a power law fit Δ of 0.69 for Sample 1 and 0.46 for Sample 2. This difference in linearity with respect to the applied electric field serves to illustrate the differences in material quality alongside the results for current with respect to doserate. This difference serves to indicate that there is a more pronounced effect limiting the velocity and effective internal field in Sample 2, and that the effect as seen in Sample 2 is subject to a greater increase with increased electric field.

2.4 Area measurement
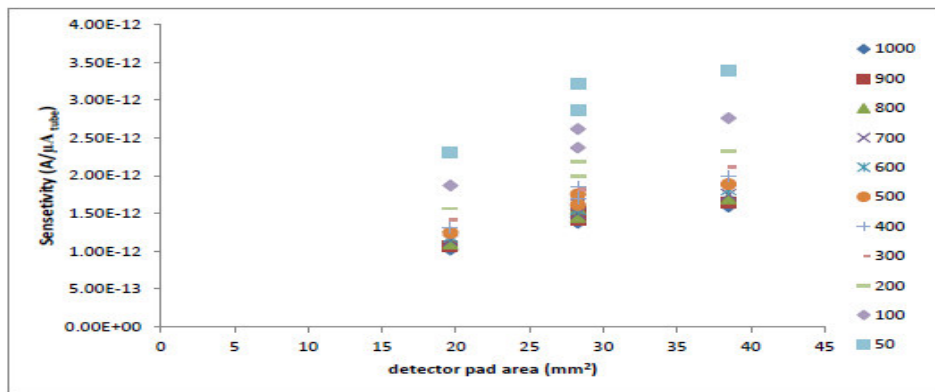
Figure 12. *Sensitivity vs. pad area Sample 1 at 120V Bias, each series corresponds to a tube current in µA.*
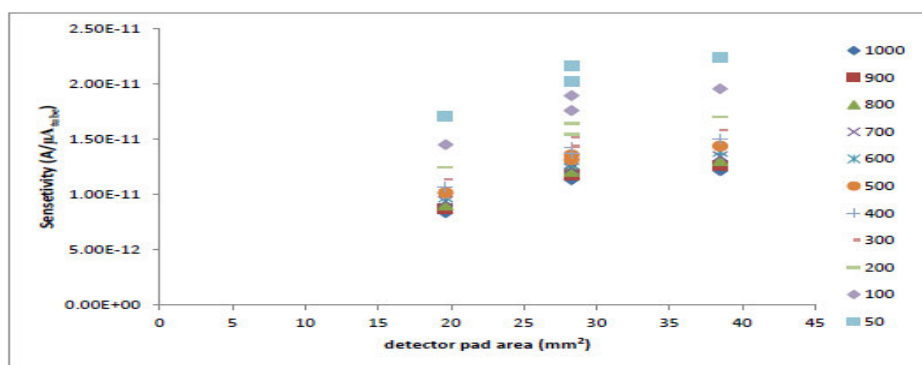
Figure 13. *Sensitivity vs. pad area Sample 1 at 6V Bias, each series corresponds to a tube current in µA.*
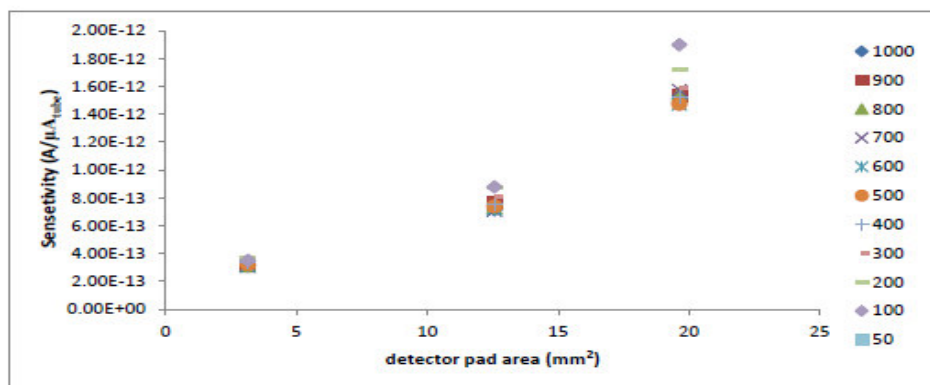
Figure 14. *Sensitivity vs. pad area Sample 2 at 200V Bias, each series corresponds to a tube current in µA.*

When the sensitivity is presented as a function of area (The sensitivity defines the expected output response from the detector for a given incident doserate) , as in Figures 12-14, the non-linearity of the response with respect to both doserate and detector pad area are apparent. At the lowest doserates there is a visible diversion in response between the two medium-sized pads, which converge in response as the doserate is increased. As can be seen, there is a clear increase in sensitivity for the lower doserates, contributing to the non-linearity in photocurrent and lower Delta value. The same results may be seen for Sample.2 as in Figure.14 with a similar non-linear relation between pad area and sensitivity. However, due to the improved linearity there is a much narrower divergence between the series corresponding to each doserate. Notable is that the apparent direction of the curve of response for each is in a different direction, though due to the limited number of directly comparable data points it is difficult to form any certain conclusions about this. From the response seen in the collimated measurements on Sample 1, where each pad had an equal sized area in roughly the centre of each pad exposed, the response was found to be independent of the pad area. This result is exactly what would be expected, as it effectively treats each of the pads as the same size. This suggests that there may be additional effects present at the edge of the detector pads that are detracting from linearity in size. If there are edge effects present then the results here may also suggest that they have some dependency on the incident doserate, due to

16

the improved dose linearity across all pads when collimation is used.

2.5   Rise Time Measurements
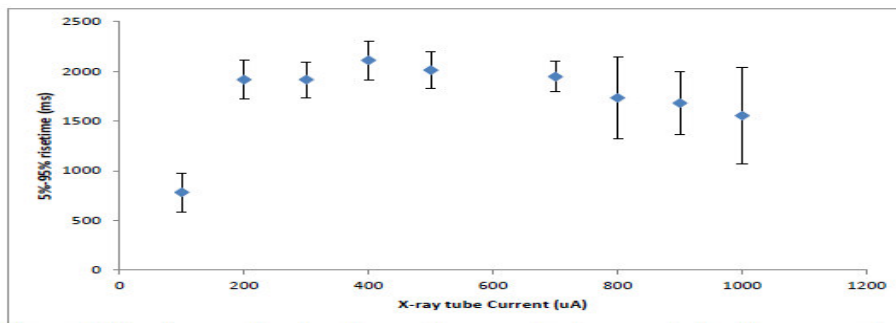
Figure 15. *Rise time as a function of x-ray tube current for the x-ray tube itself, as measured by a silicon PIN diode.*
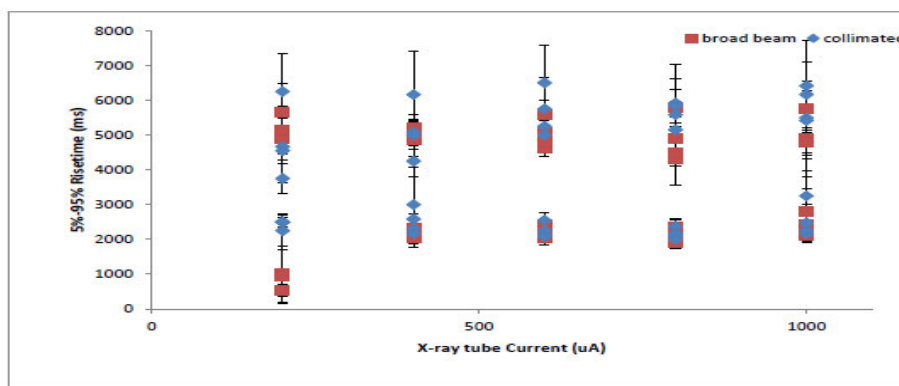
Figure 16. *Rise time as a function of x-ray tube current for Sample 1, measured across all pads at 6V and 120V bias.*
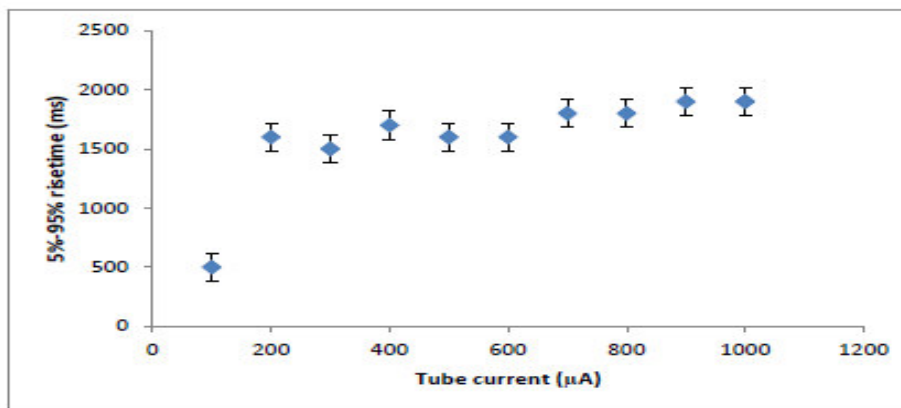
Figure 17. *Rise time as a function of x-ray tube current for Sample 2, measured across all pads at 200v bias.*
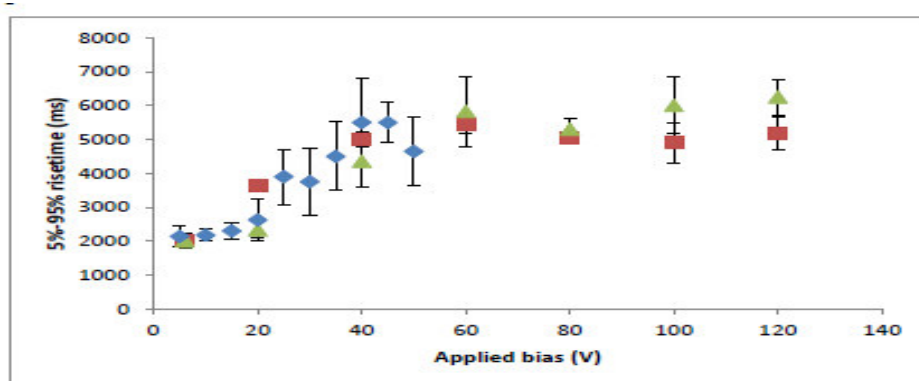
Figure 18. *Rise time as a function of applied bias for Sample 1, measured for pad C at 1000µA tube current, the different series' represent results from different sets of measurements.*
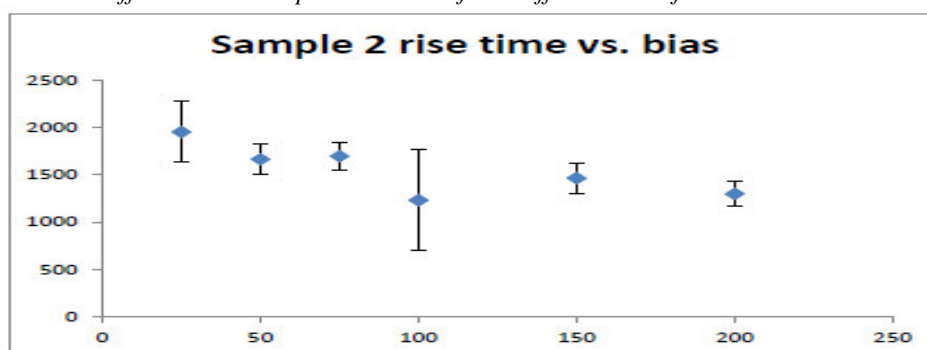
Figure 19. *Rise time as a function of applied bias for Sample 2, measured for pad F at 1000µA tube current.*
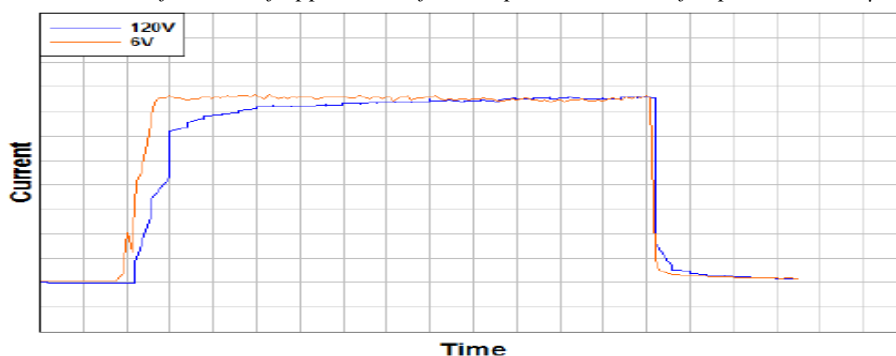
Figure 20. *Overlaid current-time traces from Sample 1 scaled to same peak magnitude.*

The results in Figures 15 to 20 show the results of the investigations into the effects of doserate and applied bias voltage on the response time of the detector. To allow compensation for its effects, the x-ray tubes own rise time, with respect, is quantified in Figure 15 at lower tube currents there was found to be an increasing rise time which stabilised at tube higher currents. This result can be used to explain the observed behaviour as seen in Figure 16, for Sample 1; the rise time is largely independent of the tube current and so doserate, with the only apparent reduction in rise time due to tube current variation coming from rise time of the x-ray tube itself. This is absolutely confirmed by the inclusion of the collimated result series, they follow exactly the same pattern and rise times with respect to tube current with the same applied bias despite their photocurrent, and so doserate being between one and two orders of magnitude less. This result also indicates an area independence to the rise time, the only factor significantly separating the various series' for Sample 1 is the applied bias. Figure 18 shows the result on the rise times from varying the bias voltage, with a fixed x-ray tube current. There is an increase in the rise time of the detector after which it appears to plateau. As shown in Figure 18, this plateau in rise time does not correspond with a plateau in the sensitivity of the device, which increases with a near linear response across the tested range. If the shapes of the transients after the tube is turned on are compared, as in Figure 20, it can be seen that there may be a relation where there is a fast initial rising component and then a second, curved component which becomes more pronounced with increasing fields up to a point. This observed undershoot that leads to the extension of rise time is often attributed to the presence of the shallow defect levels (Guerrero, M.J, et al 2006) , which may start to empty whenever the detector is not under irradiation. It is additionally known

that the efficiency of the priming effect is dependent upon the applied detector bias (Mersi, S., et al 2004), with decreasing efficiency in priming as the bias is increased. From the combination of these principals it is apparent that it will take longer for the signal which is produced by a higher voltage to overcome the signal reduction effects that will be present until the shallow traps are again filled. From this explanation, it is not apparent how there appears to be an independence between doserate and the rise time, as 10 times the dose should logically fill the same amount of now vacant traps 10 times faster. From Figure 16 there is a much wider spread in rise times seen for the 120v bias measurements than for the 6v measurements. This could be used to argue that there is some level of doserate dependence in the rise time; it is just not clear from these results. This would agree with what has been seen in the limited literature available, and that at the low bias has a sufficiently small impact on efficiency to enable even the lowest measured doserate to have saturated all the available traps in a very short space of time. This reasoning cannot easily account for the plateau in the rise times however, as the reasoning behind the increase in rise time suggests that until unless there is some manner of velocity saturation occurring, the rise time should continue to increase with field, and the maximum employed field here is likely insufficient to cause this. It is 4000V/cm with the plateau occurring at a field of 2000V/cm, significantly less than the figure of 10 kV/cm needed. There is in the literature, an alternative, extended suggestion for the nature of this process that may account for this, however. It is suggested (Bergonzo, et al 2007). that this response can be attributed to the effects of shallow trapping levels that are subject to constant thermal de-trapping, creating a reduced internal electric field that takes time to settle by priming. It also suggests that for high quality material the created charge carriers are capable of reaching the contacts within their lifetimes at higher fields, giving rise to an additional injection photocurrent. This will again take time to stabilise and is thought to be the dominant contribution to the rise time at higher field strengths. If the bias where the rise time appears to plateau is sufficient to give a charge collection distance such that this injection photocurrent becomes significant, it could possibly serve to counteract a reduction in priming efficiency from the increasing field. This addition still does not entirely account for the apparent flat response of rise time with doserate, and still requires the assumption that there may be decrease in rise time with added dose. In terms of the results for Sample 2, which exhibits an apparently flat response with respect to doserate, as in Figure 17, and a rise time that may decrease with increasing bias as in Figure 19. The theory as put forward in may best explain this. If the material has a higher concentration of defects or impurities, as would agree with the current response of the device, then it is possible that there is a more significant electric field from polarization and deep trap priming present, opposing the externally applied field, giving an effective low internal field that does not perturb the very rapid priming even at low doserates. The response with respect to the applied field can also be accounted for by considering that the larger concentration of traps will restrict the carrier mobility within the material, so leading to minimal involvement from injection currents. Additionally if there is a relatively strong internal field from polarization, the increase in the applied field may be resulting in a lower effective internal field, so agreeing with the bias rise time correlation seen in the results.

3. Conclusions

This work appears to confirm that there is an under-response to x-ray irradiation with respect to detector area in samples of diamond with a sandwich-type detector geometry. Limited testing with a collimated x-ray beam appears to suggest that it may be an edge-related effect, which is supported by the nature of the under-response and theory. To probe this further, future work could investigate the same sample but with a higher precision method of aligning fine collimated beams to look at the effect of moving a small effective pad to near the edge of each real pad and quantifying the reduction, if any, in signal magnitude as the edge is approached. Alternatively, it may be productive to simply put multiple different sets of pads of varying sizes onto this sample or another of sufficiently similar material. Additionally, it was found that by varying bias voltage, the magnitude of signal out of the detector could be improved. But at the expense of introducing a time-dependent component to the signal which has a settling time significantly longer than the effects those seen at low bias, which are close to the rise time of the x-ray tube. Further understanding into the causes and significance of these effects, time varying, could possibly be found by verifying any effects of detector area and doserate or the absence thereof. It is suspected that the main factors determining the magnitude of the effect of doserate on rise time will be material quality, with a minor doserate component, so in particular the response of rise time with bias could be examined for multiple doserates in a similar manner to the single one here. Due to issues encountered with reproducible noise effects it might be suggested that the diamond detector as tested would not be suitable for use as a dosimeter, but further studies into its behaviour may offer more useful insights for detector design, particularly the effect of the size of the contacts in the widely used sandwich-type geometry and the effects responsible for the observed varying rise time.

References

Adea, N., Nama, T.L., Derrya, T.E. & Mhlangab, S.H.(2014), The dose rate dependence of synthetic diamond detectors in the relative dosimetry of high-energy electron therapy beams, Radiation Physics and Chemistry, 98, 155–162.

Almaviva, S., Verona, C., Verona-Rinati, G., Ciancaglioni, I., Consorti, R., DeNotaristefani, F., Manfredotti, C., Marinelli, M., Milani, E., Petrucci, A. & Prestopino, G. (2009), Synthetic single crystal diamond dosimeters for Intensity Modulated Radiation Therapy applications, Nuclear Inst. and Methods in Physics Research, A, 608, 1, 191-194.

Attix, F., Roesch, W.C & Tochilin, E. (1968), Radiation Dosimetry, 1, 2nd edition, Academic Press, New York.

Bergonzo, P., Tromson, D., Descamps, C., Hamrita, H., Mer, C., Tranchant, N. & Nesladek, M. (2007), Improving diamond detectors: A device case, Diamond & Related Materials, 16, 4, 1038-1043.

Betzel, G.T., Lansley, S.P., Baluti, F., Reinisch, L. & Meyer, J. (2010), Operating parameters of CVD diamond detectors for radiation dosimetry, Nuclear Inst. and Methods in Physics Research, A, 614, 1, 130-136.

Bruzzi, M., Bucciolini, M., Casati, M., DeAngelis, C., Lagomarsino, S., Løvik, I., Onori, S. & Sciortino, S. (2004), CVD diamond particle detectors used as on-line dosimeters in clinical radiotherapy, Nuclear Inst. and Methods in Physics Research, A, 518, 1, 421-422.

Buttar, C.M., Conway, J., Meyfarth, R., Scarsbrook, G., Sellin, P.J. & Whitehead, A. (1997), CVD diamond detectors as dosimeters for radiotherapy, Nuclear Inst. and Methods in Physics Research, A, 392, 1, 281-284.

Element Six Ltd, United Kingdom, Global Innovation Centre, Fermi Avenue, Harwell Oxford, Didcot, Oxfordshire, OX11 0QR, UK. Tel: +44 1235 441000, fax: +44 1235 441001

Fowler, J. F. (1966), Radiation Dosimetry, vol 2 ed F H Attix and W C Roesch (New York: Academic), 241–324.

Guerrero, M.J., Tromson, D., Rebisz, M., Mer, C., Bazin, B. & Bergonzo, P. ,(2004), Requirements for synthetic diamond devices for radiotherapy dosimetry applications, Diamond & Related Materials,13,11, 2046-2051.

Guerrero, M.J., Tromson, D., Descamps, C. & Bergonzo, P. (2006), Recent improvements on the use of CVD diamond ionisation chambers for radiotherapy applications, Diamond and Related Materials, 15, 4–8, 811-814.

Knoll, G.F. (2010), Radiation detection and measurement, (4rd ed.). Wiley, Hoboken, N.J.(Chapter 11).

Lansley, S., Betzel, G., Baluti, F., Reinisch, L. & Meyer, J. (2011), Synthetic diamond X- ray dosimeter for radiotherapy, RADIATION MEASUREMENTS, 46, 12, 1658-1661

Lei, L., Ouyang, X., Tan, X., Xia, L., Cao, N., Liu, B. & Zhang, X. (2012), Priming effect on a polycrystalline CVD diamond detector under Co-60 gamma-raysirradiation, NUCLEAR INSTRUMENTS & METHODS IN PHYSICS RESEARCH SECTION A-ACCELERATORS SPECTROMETERS DETECTORS AND ASSOCIATED EQUIPMENT, 672, 29-32.

Manfredotti, C., Polesello, P., Truccato, M., Vittone,E., Giudice, A. Lo. & Fizzotti, F.,(1998), CVD diamond detectors, Nuclear Instruments and Methods in Physics Research Section A: Accelerators, Spectrometers, Detectors and Associated Equipment, 410, 1, 96-99.

Manfredotti, C. (2005), CVD diamond detectors for nuclear and dosimetric applications , DIAMOND AND RELATED MATERIALS, 14, 3-7, 531-540.

Manfredotti, C., Lo Giudice, A., Ricciardi, C., Paolini, C., Massa, E., Fizzotti, F. & Vittone, E. (2001), CVD diamond microdosimeters , Nuclear Inst. and Methods in Physics Research, A, 458, 1, 360-364.

Manfredotti, C. (2005), CVD diamond detectors for nuclear and dosimetric applications , DIAMOND AND RELATED MATERIALS, 14, 3-7, 531-540.

Marczewska, B., Nowak, T., Olko, P., Nesladek, M. & Waligórski, M.P.R. (2001), Studies on the application of CVD diamonds as active detectors of ionising radiation, Physica B: Physics of Condensed Matter, 308, 1-2, 1213-1216.

Mersi, S., Borchi, E., Bruzzi, M., Alessandro, R. D'., Lagomarsino, S. &Sciortino, S. (2004), A study of charge collection processes on polycrystalline diamond detectors, Nuclear Instruments and Methods in Physics Research Section A:Accelerators, Spectrometers, Detectors and Associated Equipment, 530, 146-151.

Schirru, F., Marczewska, B., Tallaire, A., Achard, J., Nowak, T. & Ko, P. (2007), Dosimetric properties of thick single CVD crystal diamonds, PHYSICA STATUS SOLIDI A-APPLICATIONS AND MATERIALS SCIENCE, 204, 9, 3030-3035.

Whitehead, A.J., Airey, R., Buttar, C.M., Conway, J., Hill, G., Ramkumar, S., Scarsbrook, G.A., Sussmann, R.S. & Walker, S. (2001), CVD diamond for medical dosimetry applications, Nuclear Inst. and Methods in Physics Research, A, 460, 1, 20-26.

The IISTE is a pioneer in the Open-Access hosting service and academic event management. The aim of the firm is Accelerating Global Knowledge Sharing.

More information about the firm can be found on the homepage:
http://www.iiste.org

CALL FOR JOURNAL PAPERS

There are more than 30 peer-reviewed academic journals hosted under the hosting platform.

Prospective authors of journals can find the submission instruction on the following page: http://www.iiste.org/journals/ All the journals articles are available online to the readers all over the world without financial, legal, or technical barriers other than those inseparable from gaining access to the internet itself. Paper version of the journals is also available upon request of readers and authors.

MORE RESOURCES

Book publication information: http://www.iiste.org/book/

Academic conference: http://www.iiste.org/conference/upcoming-conferences-call-for-paper/

IISTE Knowledge Sharing Partners

EBSCO, Index Copernicus, Ulrich's Periodicals Directory, JournalTOCS, PKP Open Archives Harvester, Bielefeld Academic Search Engine, Elektronische Zeitschriftenbibliothek EZB, Open J-Gate, OCLC WorldCat, Universe Digtial Library , NewJour, Google Scholar